The response of common carp (*Cyprinus carpio*) to insonified bubble curtains

Nicholas Flores Martin[1], Timothy G. Leighton[2], Paul R. White[2], Paul S. Kemp[1]

[1] International Centre for Ecohydraulics Research, Faculty of Engineering and Physical Sciences, University of Southampton, Boldrewood, SO16 7QF, UK

[2] Institute of Sound and Vibration Research, University of Southampton, Highfield, SO17 1BJ, UK

***** Corresponding author: nicholas.floresmartin@soton.ac.uk

Running title: Carp response to resonant acoustic bubbles

Keywords: Bubble resonance, bubble coalescence, fish screening, fish passage.

ABSTRACT

Acoustic bubble curtains have been marketed as relatively low cost and easily maintained behavioural deterrents for fisheries management. Their energy efficiency can be improved by reducing air flow and exploiting bubble resonance. In a series of three flume experiments, we: (1) investigated the reactions of carp to a low air flow bubble curtain, (2) compared the effectiveness of resonant versus non-resonant insonified bubble curtains (for the same volume flux of gas injected through the nozzles) to deter passage, and determined the stimuli responsible for eliciting deterrence, and (3) included the effect of visual cues generated by the bubble curtain. This study showed that bubble curtains with a higher proportion of resonant bubbles deterred carp relatively better. Passage rejection was likely influenced by multiple cues at distances within a body length of the fish - specifically the rate of change in both particle motion, and flow velocity caused by rising bubbles. All acoustic bubble curtains were less effective in the presence of daylight, suggesting that vision plays an important role at mediating carp reactions. We discuss the importance of ascertaining the bubble size distribution, in addition to the gas flow rate and aperture size, when characterising acoustically active bubble curtains.

I. INTRODUCTION

River off-takes that abstract and convey water to irrigation channels, hydropower turbines, power station cooling systems, or fish farms, can have multiple negative impacts on fish. Off-stream water use (e.g. irrigation) can remove fish from a population, whereas in-stream use (e.g. hydropower) can cause death, injury or delayed mortality at turbines and pumping stations (Solomon, 1992). Traditionally, physical or mechanical screens are used to protect fish at these structures, by blocking and/or guiding them to alternative, safer routes (Jansen *et al.*, 2007). When designed and operated correctly, physical screen guidance efficiencies can range between 80-100% (Turnpenny & O'Keefe, 2005; Amaral *et al.*, 2003; Inglis *et al.*, 2003). However, such methods can have several limitations often being costly to deploy and maintain, particularly when there is debris accumulation (Solomon, 1992; Turnpenny & O'Keefe, 2005), and can themselves harm fish through mechanical abrasion and impingement (Calles *et al.*, 2010). Furthermore, their effectiveness at blocking and guiding larval and juvenile life-stages can be limited as these can pass through them (Turnpenny & O'Keefe, 2005; Kemp *et al.*, 2012) or lack the swimming capability to escape once impinged (Moser *et al.*, 2014). Consequently, this had led to an interest in developing and testing non-physical guidance methods.

Behavioural guidance systems can use a diverse array of stimuli to repel and attract fish, although attractors, such as pheromones (Johnson *et al.*, 2009; Sorensen & Stacey, 2010), are less frequently used than repellents. Repellents include electric fields, e.g. Eurasian ruffe, *Gymnocephalus cernuus* (Dawson *et al.*, 2006), air bubbles, e.g. gizzard shad, *Dorosoma cepedianum* and striped bass, *Morone saxatilis* (Kuznetsov, 1971); common carp, *Cyprinus carpio* and Asian carp, *Hypopthalmichthys spp. (*Zielinski & Sorensen, 2016*);* Atlantic salmon smolts *Salmo salar* (Leander *et al.*, 2021), strobe lights, e.g. Atlantic menhaden, *Brevoortia tyrannus*, spot, *Leiostornus xanthurus*, and white perch, *Morone americana* (McIninch &

Hocutt, 1987) and continuous light, e.g. European eel, *Anguilla anguilla* (Lowe ,1952), acoustics, e.g. silver carp, *Hypopthalmichthys molitrix* (Vetter *et al.,* 2015, 2018); bighead carp, *H. nobilis* (Vetter *et al.*, 2017); various estuarine species (Maes *et al*., 2004); European eel (Sand *et al.,* 2000; Deleau *et al.,* 2019; Piper *et al.*, 2019), river lamprey (Deleau *et al.*, 2020), hydrodynamics, e.g. chinook salmon, *Oncorhynchus tshawytscha (*Enders *et al.,* 2009; Goodwin *et al.,* 2014*)*, odours of decaying conspecifics, e.g. sea lamprey *Petromyzon marinus* (Wagner *et al.,* 2011), and shade, e.g. chinook salmon (Kemp *et al.,* 2005). Efficiencies vary greatly between studies and are often much lower than those obtained for physical screens (Turnpenny *et al.,* 1998) that, as a consequence, are the preference of many regulatory agencies (Solomon, 1992; Turnpenny & O'Keefe., 2005). However based on applying the Theory of Marginal Gains to fish screening (Deleau *et al.,* 2019), where many small incremental improvements in the system amount to a significant gains when added together, there remains considerable potential for developing behavioural deterrents to enhance the performance of physical devices when used in combination.

One of the potential explanations for the lower than expected performance of behavioural deterrents is that their development has historically been unsystematic and based largely on a process of trial-and-error (Katopodis & Williams, 2012), rather than focusing on fundamental principles and an understanding that responses to stimuli vary among species, life-stage and individuals (Budaev *et al.,* 2002; Noatch & Suski., 2012). Results are often contradictory, particularly if insufficient rigour has been applied during testing (Hocutt, 1980; Noatch & Suski, 2012), and may reflect differences in site or approach adopted, e.g. field studies versus controlled experiments (Noatch & Suski, 2012; Zielinski *et al.,* 2015; Leighton *et al.,* 2020). Concerns have also been raised with regard to a lack of habituation studies (Putland & Mensinger, 2019; Popper & Hawkins, 2019), insufficient quantitative data, and use of proprietary acoustic stimuli in previous studies, precluding testing by third parties (Putland

& Mensinger, 2019). As a result, river managers and environmental engineers can receive mixed messages, and so far the use of behavioural methods to complement physical screens remains limited (Turnpenny & O'Keefe, 2005).

The efficiency of behavioural guidance devices may be improved if more than one stimulus is used in combination (Noatch & Suski, 2012). Multiple stimuli have proven more effective in studies that compared them against their constituent stimuli alone. These include strobe lights with bubbles e.g. Atlantic menhaden, spot, and white perch (McIninch & Hocutt, 1987; Sager *et al.*, 1987), alewife *Alosa psuedoharengus*, rainbow smelt *Osmerus mordax*, and gizzard shad (Patrick *et al.*, 1985), sound with electric fields e.g. Atlantic salmon (IOE Group 1994), and bubbles with broadband sound e.g. Atlantic salmon smolts (Welton *et al.*, 2002), bighead carp (Taylor *et al.*, 2005; Dennis *et al.*, 2019). It is likely that these improvements in performance are the result of using multi-modal cues operating via different sensory systems in which stimuli can either act independently, or where one stimulus improves responsiveness to another (Vowles & Kemp, 2012; Vowles *et al*., 2014).

Insonified bubble curtains (i.e. bubble curtains driven by a sound field) present multi-modal acoustic, hydrodynamic, and visual stimuli. Bubbles introduced underwater generate sound and create turbulence that is influenced by bubble density and rise velocity (Brevik & Kristiansen, 2002). Furthermore, they can create a visual barrier by obscuring a fish's line of sight (Flammang *et al.*, 2014; Stewart *et al.*, 2014), although guidance efficiencies are generally higher at night for species such as walleye *Sander vitreus* (Flammang *et al.*, 2014), muskellunge *Esox masquinongy* (Stewart *et al.*, 2014), largemouth bass *Micropterus salmoides* (Lewis *et al.*, 1968), and sockeye salmon *Oncorhynchus nerka (*Brett & MacKinnon, 1953*)*. This might be because fish can detect gaps during daylight hours through which they can pass, as suggested for Atlantic salmon smolts (Welton *et al.*, 2002). Despite these examples, few studies account

for the influence of visual cues when quantifying the guidance efficiencies of behavioural deterrents.

Although insonified bubble curtain deterrents are commercially available and can, attain high levels of efficiency (e.g. Welton *et al.,* 2002; Taylor *et al.,* 2005; Dennis *et al.,* 2019), there is potential to improve their cost-effectiveness. Reductions in air flows to below those recommended in industry best practice guidance (60 - 240 L min^{-1} m^{-1} of bubbler length) could save power, which although not a trivial challenge, could be achieved by exploiting the little-explored fundamental principles of bubble resonance and coalescence. When driven by an external sound field, a bubble will extract energy from it and pulsate, in the process radiating some energy while the remaining is ultimately converted to heat through viscothermal processes in the gas and liquid. However, if the size of the bubble is such that the frequency of the sound field causes the bubble to pulsate close to resonance, then this effect is magnified resulting in greater absorption of the sound, and a local resonance peak in scattering (Leighton, 1994). This property can be used to trap sound between bubble plumes of a size tuned to the sound field, creating a sharper sound gradient, and potentially improving the effectiveness of the insonified bubble curtain.

The control of the size of bubbles generated is challenging at high flow rates, such as those typically used in industry, because of bubble coalescence. A commonly used method to control bubble size is to change the aperture of the orifice used to introduce air underwater (e.g. Zielinski *et al.,* 2014). This is ineffective because when a series of air bubbles are introduced underwater these will tend to merge with growing successor bubbles at the nozzle, creating a bubble with a diameter much larger than that of the orifice (Leighton *et al.*, 1991). This process occurs unpredictably, leading to the production of a wide distribution of bubble sizes, and its effect increases with air flow (Leighton *et al.,* 1991). Although this problem can be mitigated

by substantially reducing the airflow to generate a more consistent bubble size, this reduces the throughput of gas, requiring more orifices, and has a limited effect for bubbles much smaller than approximately a millimetre diameter (Leighton *et al.*, 1991). Leighton *et al.*, (2012) demonstrated how the mass flux of gas through a needle could be made to deliver varying but controllable changes to the acoustic absorption, by vibrating the needle with a mobile phone vibrator. This allows the control of bubble size for the same volume of gas flowing through it by preventing coalescence. Vibrating the nozzles at different rates while using identical apertures and gas fluxes allows for the generation of bubble clouds with distinct characteristics. This method was applied in this study to test how changing bubble size distribution can influence the acoustic effects of the bubble curtain and its effectiveness as a deterrent.

This study investigated the potential of resonant acoustic bubble curtains to deter fish, comparing to what extent control of the bubble size can cause changes in the sound field. . The objectives, which built progressively on each other, were to: (1) test the reactions of fish to a bubble curtain that uses a lower air flow than those found in the literature, (2) compare the effectiveness of resonant versus non-resonant insonified bubble curtains to deter passage, using identical gas volume flow rates through the same set of injectors, and determine the stimuli responsible for eliciting this response, and (3) include the effect of visual cues generated by the bubble curtain by quantifying fish response to insonified bubbles under conditions of daylight and darkness.

II METHODS

To achieve the objectives set, three experiments were conducted to investigate carp response to: a bubble curtain generated by low air flow (Experiment 1); resonant and non-resonant insonified bubbles (Experiment 2); insonified bubbles in the presence and absence of visual cues (Experiment 3).

A. Experimental setup

All experimental trials were conducted using an annular raceway at the International Centre for Ecohydraulics Research (ICER) research facility, Southampton Science Park (Fig. 1). The channel (1.0 m wide) contained still, conditioned tap water (0.60 m deep). An experimental section (8.0 m total length) was separated from the rest of the channel by wooden framed polyester mesh barriers (1 cm mesh size). Four underwater cameras were suspended to just below the water surface. Each had an effective field of view of 60 x 60 cm of the channel floor that overlapped to ensure complete coverage of the approach to a bubble curtain and sufficient to capture all rejection responses since tracking data revealed that 95% occurred within 30 cm of the bubble curtain, and none further than 41 cm. To control for visual cues in Experiments 1 and 2, trials were conducted under conditions of darkness during the night only with the experimental area illuminated by infra-red light (850 nm) units so that fish behaviour could be recorded. Visual cues were accommodated in Experiment 3 by conducting the trials during both day and night, illuminated by daylight and infra-red lighting, respectively. The raceway was covered by a sheet of tarpaulin to prevent any natural or artificial sources of light affecting the experiment. Luminous flux was measured using a Di-log 7030N with peak sensitivity of 550 nm and sensitivity range of 500 – 625 nm (night trials: 0.0 – 0.02 Lux / 0.0 - 0.0002 Wm^{-2}; day trials: 105 – 3306 Lux / 0.91 – 28.5 Wm^{-2}).

In Experiment 1, the bubbler was constructed from two rows of 38 mm grey PVC piping, with 3 mm holes drilled at 5 mm intervals. The two rows were 15 cm apart. A total of 36 gauge 21 (38.1 mm length, 0.8 mm internal diameter) hypodermic needles were used as injection nozzles connected to each hole. Air (at 60 L min^{-1} , pressure: 1 bar, or 30 L min^{-1} m^{-1} of bubbler) was supplied to the bubbler via 6.4 mm ID nylon tubing leading to a compressor (Clarke Bandit, 1HP), and flow monitored with an air flow meter (IDS, MR3000).

An insonified bubble curtain was used in Experiments 2 and 3 (Fig. 1). The bubble curtain consisted of two bubble clouds, one on either side of an Electrovoice UW-30 underwater speaker. Bubbles were generated using a device consisting of 18 linearly arranged, horizontal, gauge 21 needles secured using luer-to-barbed adaptors (Cole Parmer, WZ-45518-46), and housed within modified lengths of plastic trunking (FIG. 1) (See supplementary material at [URL will be inserted by AIP] for photograph of the device). Air supply (at 2 bar) was provided individually to the needles, via manifold air tubes (4 mm ID silicone), and 6.4 mm ID nylon tubing leading to a compressor (Clarke Bandit, 1 HP). Fine-scale control of air flow was ensured by using a three-way pressure reducing valve (Honeywell, PRV) and air flow meter (IDS, MR3030). Vibration of the nozzles was provided by a total of 36 haptic feedback motors, one of which was attached to each injection nozzle (Precision microdrives, 307-103). Adjusting the voltage supplied to the motors allowed control of the magnitude of the vibration. To protect the fragile flying leads, each motor was placed within a custom-made 3D printed cylindrical housing and sealed in potting compound. Power was provided by two 30 V / 3 A DC Power blocks (Isotech, IPS 303DD). Each motor was connected in parallel using a series of terminal blocks.

For Experiment 2, two bubble populations were generated by injecting air (air flow: 6 L min^{-1}, or 3 L min^{-1} m^{-1} of bubbler) through nozzles with or without vibration at 3V. The two bubble clouds were either insonified by a 1750 Hz (144 dB re 1 µPa at 1 m) or a 4000 Hz (151 dB re 1 µPa at 1 m) continuous pure tone signal, each frequency driving one population to resonance. For Experiment 3, two bubble populations were generated by injecting air (air flow: 10 L min^{-1}, or 5 L min^{-1} m^{-1} of bubbler) through nozzles with or without vibration at 2.2 V. The bubbles were insonified by a continuous 1000 Hz pure tone signal at a source level of 140 dB re 1 µPa at 1 m. Frequencies were chosen after characterising the bubble size distributions for each population, after which Minnaert's (1933) equation, which relates bubble radius to resonance

frequency, was used to calculate a frequency most likely to drive significant proportions of bubbles to resonance. A single insonifying frequency was considered adequate because although complex sounds are more effective than pure tones at deterring carp (Vetter *et al* 2015), bubble curtains are sources of multiple stimuli including broadband sound (Zielinski & Sorensen, 2016). By placing the speaker between the two bubble clouds as opposed to within them, the acoustical loading on the speaker was not changed so greatly by the bubbles, and the field it initially radiated would be less affected by the bubble size produced.

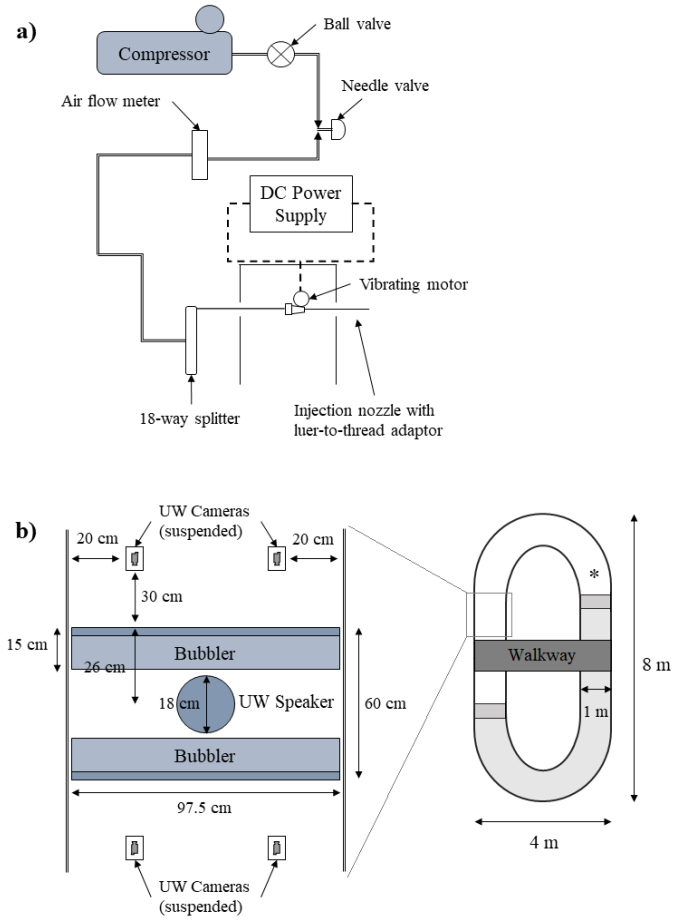

FIG. 1 (a) Schematic of the bubble curtain and air supply system used for Experiments 2 and 3 of a study to investigate the response of common carp to insonified bubble curtains in the presence and absence of visual cues. A single needle is shown for simplification, all needles were at the same depth. (b) Plan of the experimental set-up used in Experiments 2 and 3. Grey areas indicate the section of flume not used in the experiment, dark grey blocks indicate mesh

barriers. The asterisk indicates the release point for fish at the start of each trial. Set-up was asymmetrical due to presence of a walkway, although attempts and passage efficiency did not differ with side of approach.

B. Bubble sizing

To characterise the size distribution of the bubble populations, a short length of the bubbler used for Experiments 2 and 3 was tested in a glass tank (length: 80 cm; height: 40 cm; width: 40 cm). The size of the bubbles generated for fluxes equivalent to 6.0, and 10 L min^{-1} were determined at a pressure of 2 bar for vibration intensities of 0 V, 2.2 V, and 3 V (Fig. 2). For each set-up, five high-speed (1/800 s) photographs of the bubble streams were taken using a digital single-lens reflex (DSLR) camera with a macro lens, and processed in Fiji (https://imagej.net/Fiji) (See supplementary material at [URL will be inserted by AIP] for original high-speed frames at 6 L min^{-1}).

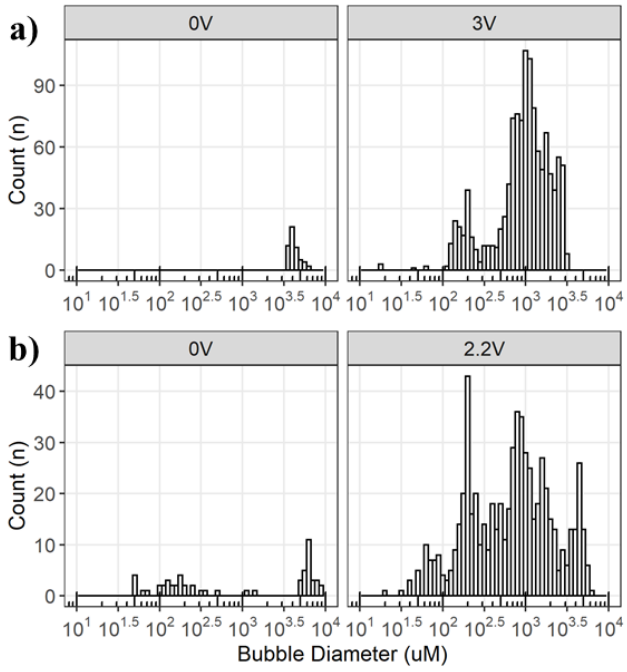

FIG. 2. – Distribution of bubble diameters (μm) at (a) 6 L min^{-1}, with standard injection (0 V), and vibration at 3 V; and (b) 10 L min^{-1} with standard injection (0 V) and vibration at 2.2 V. When the vibrating motors were activated, the general increase in bubble counts for the same

volume gas flux was because the gas was distributed in more, smaller bubbles. Note that the volume of gas in the largest non-vibrating bubble peaks (diameters $>10^{3.5}$ microns for [a] and $>10^{6}$ microns for [b]) disappeared when vibration (3 V) was activated, and these peaks contained the bulk of the gas.

C. Determination of extinction cross-sections

The interaction of an acoustic field with an object, such as a bubble, can be characterised by three related quantities: the scattering (σ_s), absorption (σ_a), and extinction (σ_e) cross-sections. The σ_s and σ_a are defined as the ratio of the power scattered or absorbed by a single bubble, divided by the intensity of an incident plane wave, and have dimensions of area. The ratio of the rate of energy loss by all mechanisms to the intensity of that incident plane wave is σ_e such that $\sigma_e = \sigma_s + \sigma_a$ (Ainslie & Leighton, 2009). To identify the bubbles with the greatest acoustic effect in each population, the extinction cross-sections (σ_e) were determined for the bubble distributions in Experiments 2 and 3, for incident sound fields of 1000 Hz, 1750 Hz, and 4000 Hz.

Here, equations (37) to (39) and (42) to (44) from Ainslie and Leighton ((2011), based on work by Andreeva (1964) and Weston (1967), were used to calculate the damping factors (Q_{vis}, Q_{rad}, Q_{th}), and cross-sections (σ_s and σ_e), respectively (See supplementary material at [URL will be inserted by AIP] for details of theory and equations used). For each bubble population, the range of bubble size diameters at which the central 90% of attenuation occurs, σ_e^{90}, was then determined (Fig. 3). This provided theory to explain the observed acoustical effects when identical volumes of gas are split between bubbles of different sizes (See supplementary material at [URL will be inserted by AIP] for modelled theoretical extinction coefficients of one bubble of each size for each frequency).

D. Mapping of stimuli

The acoustic spectra generated by the bubble curtains, speaker and vibrating motors alone, and all bubble/sound treatments used for Experiments 2 and 3 were recorded at a range of 1 m (See supplementary material at [URL will be inserted by AIP] for recorded acoustic spectra). For Experiment 2, the Sound Pressure Level (SPL) and Particle Displacement (PD) were mapped

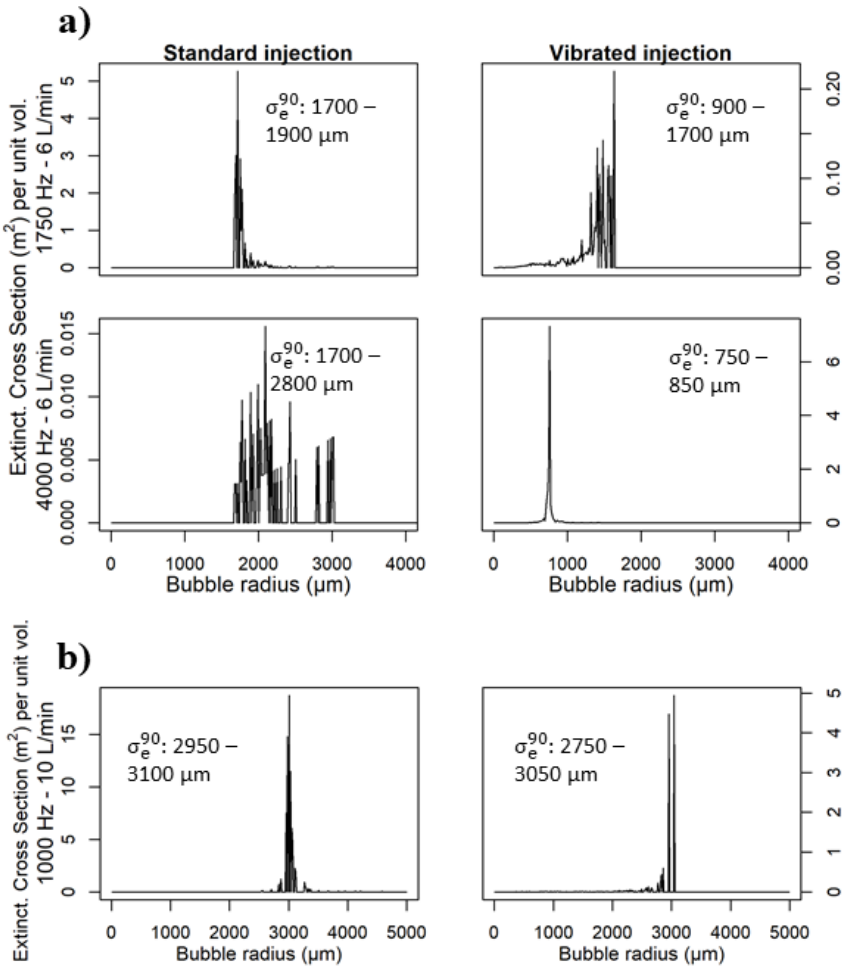

FIG. 3. – Modelled extinction cross sections for bubble distributions determined for Experiments 2 and 3: (a) an air flow of 6 L min^{-1} insonified at either 1750 Hz or 4000 Hz, with either standard injection or vibration at 3 V, and (b) an air flow of 10 L min^{-1} insonified at 1000 Hz with standard injection or vibration at 2.2V. σ_e^{90} represents the range of bubble diameters at which the central 90% of the attenuation occurs. The populations with a higher proportion of bubbles at resonance with the sound field are: 1750 Hz standard injection, 4000 Hz vibrated injection, 1000 Hz standard injection.

284 at depths of 15, 30, and 45 cm on a square grid of points with a 10 cm spacing up to a distance
285 of 1 m from the speaker (See supplementary material at [URL will be inserted by AIP] for full
286 acoustic maps including vibrating motors). SPL measurements were made with a Brüel and
287 Kjær 8103 hydrophone and pre-amplifier (Teledyne Reson VP2000). The signal was sampled
288 at 44.1 kHz, using a USB 6341 data acquisition board (National Instruments, Austin, US). Data
289 acquisition hardware was controlled using a Labview virtual instrument (Labview 2017 64-bit,
290 National Instruments, Austin, US).

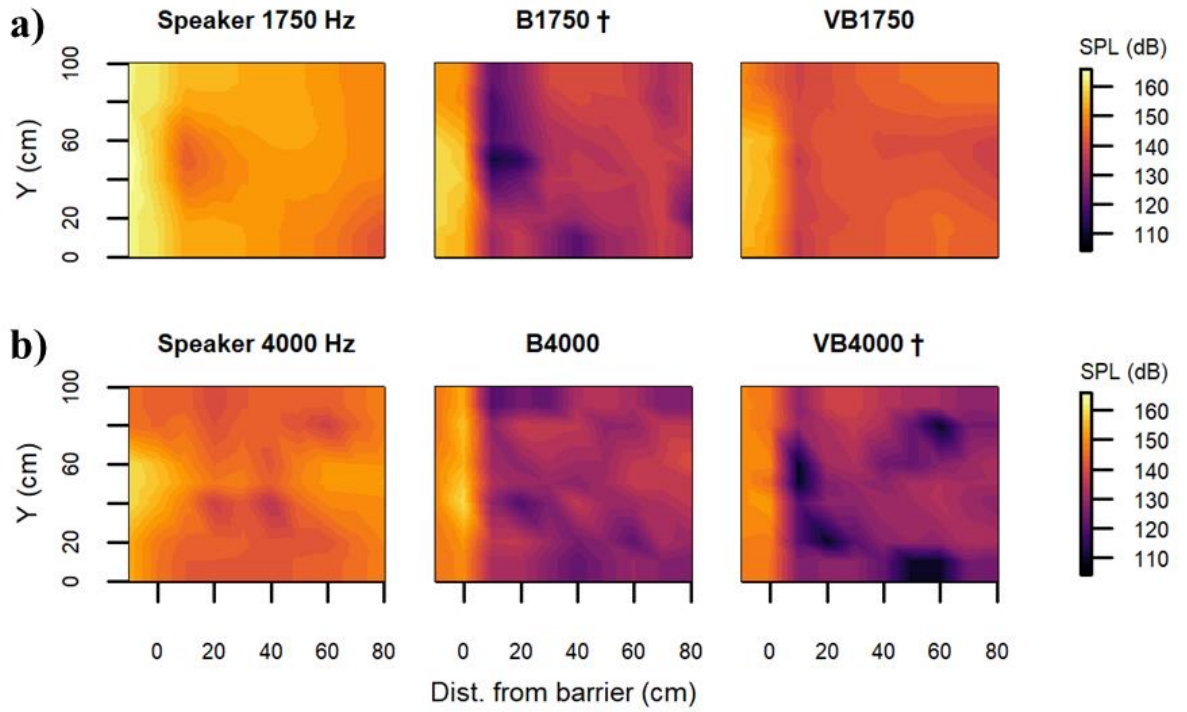

291

292 FIG. 4. – (Colour online) Acoustic maps at 45 cm depth for: (a) 1750 Hz bubble set-ups; (b)
293 4000 Hz bubble set-ups. Resonant treatments are marked by a dagger (Experiment 2). B =
294 standard injection, VB = vibrated injection. On this scale the nearest edge of the loudspeaker
295 is at horizontal position -17 cm, and the centre of the speaker at horizontal position -26 cm.
296 Sound maps of the speakers alone were included to illustrate the strong attenuating effect from
297 the bubbles.

298

PD measurements were taken using four Brüel and Kjær 8105 hydrophones arranged tetrahedrally within a custom-built aluminium frame (See supplementary material at [URL will be inserted by AIP] for assembly drawing of tetrahedral frame used to make particle displacement measurements), based on a set-up first proposed by Hickling & Wei (1995). Labview was used to record the magnitude and phase (relative to one reference hydrophone) at each hydrophone. Measurements were taken at the driving frequency for the acoustic-bubble curtains, and at the peak frequency (400 Hz) for the vibrating motors. The discretised form of Euler's equation (Zeddies *et al.*, 2010), in a single dimension, was used to determine particle velocity in the x, y, and z coordinates:

$$\frac{P_1 - P_2}{\rho_0 d} = \frac{\partial u}{\partial t} \qquad \text{where: } P_1 = Ae^{i\emptyset} \qquad (1)$$

where P_1 and P_2 are the complex amplitudes measured at two points on the same plane, separated by distance d, A is the zero-to-peak amplitude, ϕ is the phase angle, and u is the velocity in-line with the two points. The PD was derived by dividing particle velocity with the square of the angular frequency, $(2\pi f)^2$.

The hydrodynamic field around the bubble cloud was quantified. Bubbles interfere with acoustic doppler-based instruments, so an electromagnetic flow meter (Valeport model 801, Valeport, Totnes, UK) was used to measure unidirectional velocity. Measurements were taken at 60% of the depth (36 cm from the surface) at 10 cm intervals up to a distance of 1 m from the speaker. To quantify the turbulent flow induced by rising bubbles, the Standard Deviation of the flow velocity (*S.D. flow*, m/s) was used.

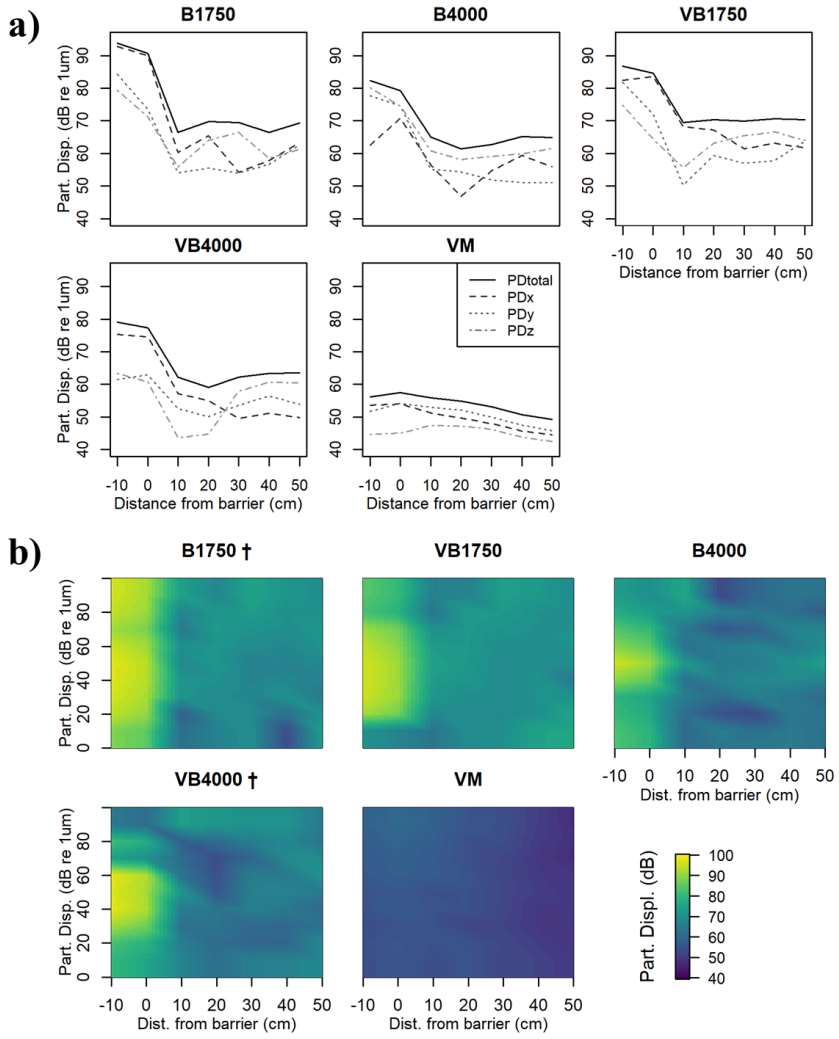

320

321 FIG. 5. – (Colour online) Particle displacement in the: (a) x y z direction, and (b) maps at 20
322 cm depth. Resonant treatments are marked with a dagger (Experiment 2). B = standard
323 injection, VB = vibrated inection, VM = vibrating motors, and numbers refer to frequency of
324 the sound field.

325 **E. Subject fish**

326 Common carp, a species with a connection between the swim bladder and hearing organs and
327 known to be deterred by bubble curtains[10], was used as the model in this study. Fish were
328 obtained from a hatchery in Hampshire, UK, and transported to ICER in well-oxygenated
329 water, and held in 3,000 L holding tanks containing well-aerated and filtered water under

ambient temperature. Water quality was checked daily and maintained at optimum levels ($[NH_4^+] < 0.125$ ppm; $[NO_2^-] < 0.25$ ppm).

At the end of each trial the subject fish were euthanized in accordance with Schedule 1 of the Animals (Scientific Procedures) Act 1986, and individual total body length (± 0.5 mm) and mass (± 0.05 g) recorded. Mean values were similar between experiments (Table I).

Experiment 3 was conducted with smaller fish, and water temperatures were lower than the previous experiments. Mean swimming velocity ±SE was higher in Experiment 2 (0.099 ms^{-1} ± 0.0007) than Experiment 3 (Mean: 0.068 ms^{-1} ± 0.0006, Day: 0.098 ms^{-1} ± 0.0011, Night: 0.057 ms^{-1} ± 0.0005). The number of approaches per hour did not vary considerably between Experiment 2 (34.43 hr^{-1} ± 2.49) and Experiment 3 (Mean: 36.40 hr^{-1} ± 1.89, day: 37.56 hr^{-1} ± 3.55, night: 35.28 hr^{-1} ± 1.65). All experiments were analysed separately, with results compared only within the same experiment.

TABLE I. Mean length, weight, and holding tank temperature for common carp used in the three experiments to investigate their response to insonified bubble curtains.

Experiment no.	Date	Mean (±SE) length (mm)	Mean (±SE) weight (mm)	Mean (±SE) tank temp. (ºC)
Experiment 1	July 2017	117.6 (21.8)	25.2 (17.5)	17.9 (0.02)
Experiment 2	July 2018	116.1 (0.7)	23.1 (0.5)	20.7 (0.3)
Experiment 3	Feb 2018	97.6 (0.6)	17.0 (0.4)	5.4 (0.4)

F. Experiments

For each experiment, trials were conducted using groups of three similarly sized naïve individuals to enable shoaling behaviour typically exhibited by this species in the wild (Huntingford *et al.*, 2002; Sisler & Sorensen, 2008; Bajer *et al.*, 2010). Prior to each trial, fish were carefully removed from the containers using a hand net and transferred to the experimental channel. The fish were allowed to acclimatise by swimming freely in in the experimental area for 15 minutes prior to each trial commencing. Movement during trials was due to volitional behaviour.

1. Experiment 1 - reactions of common carp to a bubble curtain generated by low air flow

Trials took place at night (between the end of civil dusk: 21:45 to 21:20 and start of civil dawn: 03:40 to 04:50) between 20 July and 10 August 2017. The experiment comprised two treatments, the first consisting of 12 trials with the compressor switched on but unconnected to the bubbler (control), and the second consisting of 10 trials in which the bubble curtain was active (treatment). After the initial acclimation period, all 22 trials consisted of a test (control or treatment) immediately followed by a post-test phase, each lasting 20 minutes.

2. Experiment 2 - Comparing fish response to resonant and non-resonant bubble curtains

A total of sixty 80 minute trials were conducted at night (between the end of civil dusk: 20:45 to 21:15, and start of civil dawn: 03:40 to 04:50) between 1 and 22 August 2018. The experiment comprised 5 treatments: (a) 1750 Hz, standard injection (B1750, resonant), (b) 4000 Hz, vibrated injection (VB4000, resonant), (c) 1750 Hz, vibrated injection (VB1750, non-resonant), (d) 4000 Hz, standard injection (B4000, non-resonant), and e) vibrating motors only (VM). After the initial acclimation period, twelve replicate trials were conducted for each

371 treatment, each consisting of a 40 minute pre-test (control) phase immediately followed by a
372 40 minute test.

373 ### *3. Experiment 3 – influence of visual cues on fish response to an insonified*
374 ### *bubble curtain*

375 To investigate the influence of visual cues, a total of twenty-four 45 minute trials were
376 conducted during hours of daylight (light) and a further twenty-four between the end of civil
377 dusk (18:02 to 18:23 hrs) and midnight (dark) on the 16 to 28 February 2018. Trials were held
378 during the day to more accurately represent a situation in the field. This experiment comprised
379 8 replicates of three treatments: a) injection with no vibration (i.e. standard injection), b)
380 vibrated injection, c) no injection, but vibrating motors switched on. After the period of
381 acclimation, the trials consisted of successive phases defined as a pre-test (control), test
382 (treatment), and post-test (control), each lasting 15 minutes.

383 ## G. Behavioural and statistical analysis

384 Video recordings were analysed to quantify common carp response to the insonified acoustic
385 bubble curtains. Data were evaluated in three steps: (1) coarse-scale passage and rejection
386 counts, (2) analysis of fish movement and orientation (sinuosity, swimming velocity, and
387 angular dispersion), and (3) fish response (binned rejection counts) relative to the gradients of
388 the stimuli generated by an acoustic bubble curtain.

389 ### *1. Coarse-scale passage and rejection*

390 For all experiments, and for each trial, the following coarse-scale metrics were recorded per
391 individual fish: (1) *Number of approaches* to the bubble curtain, deemed to have occurred when
392 a fish entered the visual field of the cameras, (2) *Number of passes*, and (3) *Number of*
393 *rejections*, based on whether or not an approach culminated in the fish passing through the
394 bubble curtain. A rejection was defined as a change in direction of the swimming trajectory

395 greater than 90º, followed by sustained swimming away from the bubble curtain and out of the
396 field of view. For each trial, the *Number of approaches* and *Number of passes* recorded were
397 used to calculate the *Passage efficiency*, defined as the number of successful passes expressed
398 as a proportion of the total number of approaches. As the majority of *approaches* (72 to 90%)
399 were made by solitary fish, rather than by a shoal, to simplify our analysis possible group
400 effects were ignored.

401 ***2. Fish movement and orientation***

402 For Experiments 2 and 3, swimming trajectories were determined for each approach by
403 evaluating the position of the fish every fifth frame (450 ms) using Logger Pro (Vernier, USA).
404 The resolution was sufficient to build a history of the position of the fish, rather than track
405 movements such as startle response to a sound source that was switched on. For every time
406 step the following variables were recorded: *swimming velocity*, *step length* (i.e. the distance
407 between the location of the fish every fifth frame), *relative turning angle* (i.e. the change in the
408 bearing of the fish between two points), and *Euclidean distance from the bubble curtain* (i.e.
409 the smallest distance between the fish and the bubble curtain). For approaches ending in a
410 successful pass, the trajectories of fish before and after passage were analysed separately due
411 to marked differences in directionality. Rejection tracks were also divided into two sections
412 separated by the point of rejection, that is, the point after which fish showed directed and
413 sustained swimming away from the bubble curtain for more than one body length.

414 For approaches ending in a pass, the data collected were used to calculate indices of
415 *Sinuosity (*Bovet & Benhamou, 1998; Benhamou, 2004*)*. For approaches ending in a rejection,
416 turning angles were binned at 5 cm intervals from the bubble curtain, and circular statistics
417 used to calculate the mean angle, circular standard deviation, and mean vector, *r*, or *Angular*
418 *dispersion* (Batschelet, 1981). The Rayleigh test was used on each group of binned turning
419 angles to test whether they differed from random ($p < 0.05$) (Batschelet, 1981).

3. Response to stimuli generated by bubble curtains

Using data from Experiment 2, the relationships between fish trajectories and components of the stimulus: sound pressure level (SPL, dB re 1 μPa), particle displacement (PD, dB re 1 nm), and SD flow (m s^{-1}) generated by the insonified bubble curtain were analysed.

To determine whether SPL, PD or SD flow may act as thresholds for change in behaviour, the level of each at the fish's location was calculated for each time step using a custom Python script (Python v.3.7.3) in Ubuntu (Ubuntu v.18.04.2 LTS). For each time step, the gradients for the stimuli (ΔSPL, ΔPD, ΔSD Flow) to a virtual point one body length directly ahead of the fish were determined. The *Number of rejections* were binned at 5 cm intervals and the gradients within each interval averaged.

4. Statistical analysis

Coarse-scale and sinuosity data were tested for normality and homogeneity of variance using Shapiro-Wilk and Levene's tests. When these assumptions held, data were tested using two-way Anova with post-hoc Tukey HSD tests. Otherwise, a Kruskal-Wallis test with post-hoc Dunn Tests and Bonferroni corrections was used.

For Experiment 2, GAMs with root-transformed gamma distributions were used to examine the relationship between the gradients of each stimulus, treatment, and phase on *Angular dispersion* and *Swimming velocity*. For Experiment 3, generalised additive models (GAMs) were used to model the relationship between time of day (i.e. day or night), distance from the bubble curtain, direction (i.e. towards or away from the bubble curtain, prior to or after a *Pass* or *Rejection*), treatment, and phase (i.e. pre-treatment, treatment, post-treatment) on *Angular dispersion* and *Swimming velocity*, due to their non-linearity. Starting from a saturated model, stepwise deletions were performed to identify non-significant terms, and model selection was based on residual deviance and the lowest Akaike Information Criterion

444 (AIC). The minimum adequate model was arrived at as the most parsimonious models with
445 lowest AIC value (Burnham & Anderson 2002).

446 Finally, multiple regression with stepwise selection was used to test the relationship
447 between the binned *Number of rejections* and stimuli gradients (ΔSPL, ΔPD, ΔSD Flow).

448 ## III Results

449 ### A. Experiment 1: reactions of common carp to a bubble curtain in the absence
450 ### of visual cues

451 *Number of passes* were lower in the presence of the bubble curtain than during the post-test
452 control ($F = 7.65$, $p < 0.01$, p-adj < 0.01). Consequently, *Passage efficiency* was 47% lower in
453 the presence of the bubble curtain ($F = 4.44$, $p < 0.01$, p-adj < 0.01) as a result. There was no
454 difference in the *Number of passes* between the control and the post-test control (p-adj = 0.99).
455 When the bubble curtain was operating, carp tended to pass it via a 7.5 cm gap at the flume
456 wall, and the proportion of passes at the wall was higher when the bubble curtain was in
457 operation compared to the two controls ($\chi^2 = 23.18$, $p < 0.01$).

458 ### B. Experiment 2: comparing fish response to resonant and non-resonant bubble
459 ### curtains

460 The *Number of passes* were lower during the period when fish encountered an acoustic bubble
461 curtain with a 6 L min^{-1} m^{-1} airflow, compared to the pre-test control (*Experimental phase*: $F =$
462 61.46, $p < 0.01$; *treatment:* $F = 3.27$, $p = 0.014$ - Fig. 6). The *Number of passes* was lower for
463 both resonant (B1750 and VB4000) and one of the non-resonant treatments (VB1750) (*p-adj*
464 = 0.014, < 0.01, < 0.01 respectively) than for the pre-test control. Compared to the control, the
465 two resonant treatments reduced the *Number of passes* by 65%, 45-50% for non-resonant
466 treatments (B4000, VB1750), and 30% for vibrating motors alone ($F = 4.20$, $p < 0.01$).

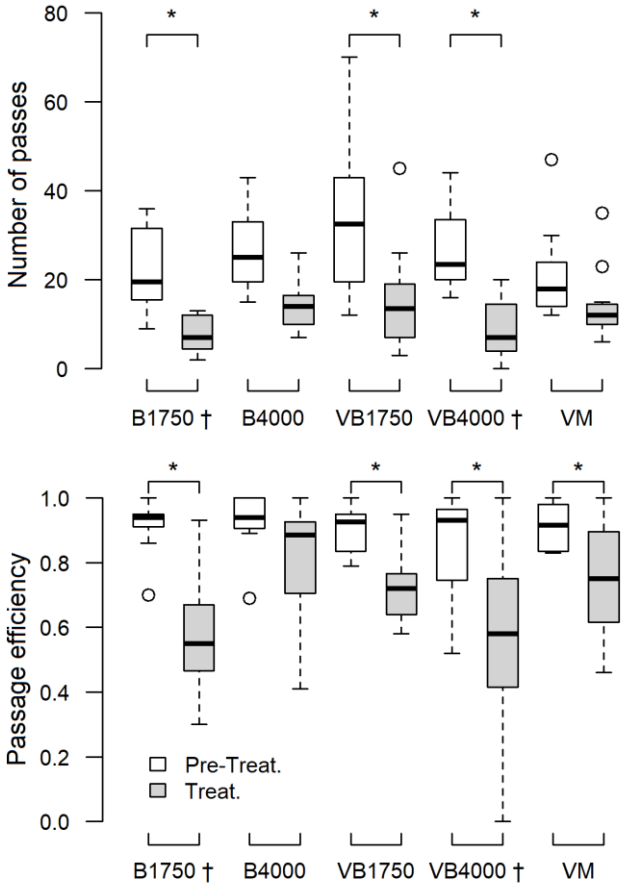

467

468 FIG. 6. – The median, interquartile range and minimum/maximum whiskers of the *Number of*
469 *passes* and *Passage efficiency* for all treatments for the 6 L min^{-1} bubble curtain during pre-
470 treatment and test periods. Pairs where a significant difference was determined are denoted by
471 an asterisk. Resonant treatments are marked by a dagger. B = standard injection, VB = vibrated
472 injection, VM = vibrating motors, and numbers refer to frequency of the sound field.

473 However, the differences between resonant and non-resonant treatments were not
474 significant, with a significant difference observed only between the two resonant treatments
475 and the vibrating motor control (p-adj = 0.013 and 0.011, respectively). *Passage efficiency* was
476 lower for all treatments compared to the pre-test control, with the exception of B4000 (B1750:
477 $\chi^2 = 15.27$, $p < 0.01$; VB1750: $\chi^2 = 11.25$, $p < 0.01$; B4000: $\chi^2 = 3.59$, $p = 0.06$; VB4000: $\chi^2 =$
478 5.63, $p = 0.018$; VM: $\chi^2 = 5.92$, $p = 0.014$).

The *Number of rejections* correlated with the gradient of all three stimuli ($F_{3,46}$ = 9.30: $p < 0.01$ - Fig. 7), and stepwise selection determined that the most parsimonious model was the one that excluded the sound pressure gradient term. Post-hoc modelling of the stimuli gave information on the individual contributions of each stimulus to the model (ΔSPL: $F_{1,48} = 11.59$, $p < 0.01$; ΔPD: $F_{1,48} = 24.35$, $p < 0.01$; ΔSD Flow: $F_{1,48} = 6.75$, $p = 0.015$ – Fig. 8). Visual inspection of the maps of SPL, and density maps of location of rejection showed that fish tended to switch direction and swim away from the bubble curtain in zones with the lowest SPL and PD, i.e. regions with the highest gradients.

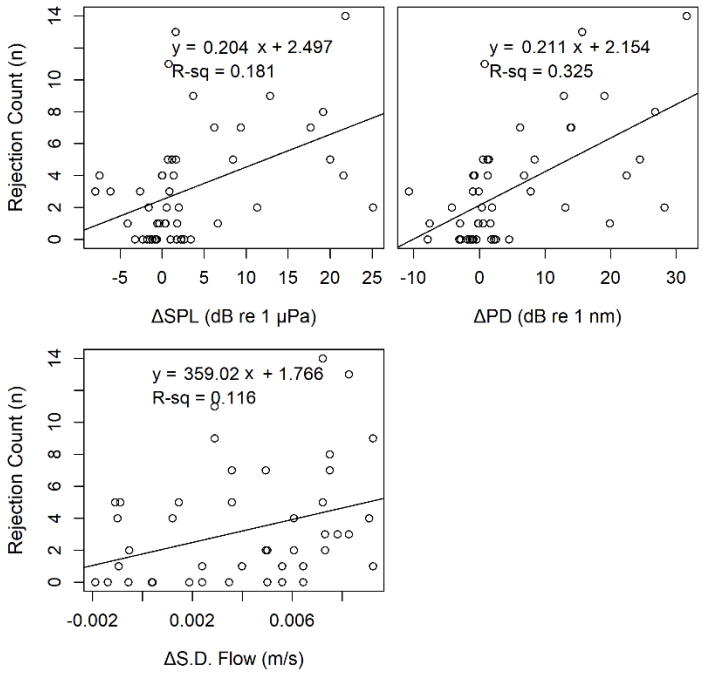

FIG.7. – Rejection counts against gradients (averaged for 10 cm bins) of all three stimuli generated by the bubble curtains.

For fish that successfully passed during the treatment phase, *Sinuosity index* values were higher on approach to the bubbler compared to when swimming away (Fig. 8). These differences were not observed during the pre-test control period (B1750 $\chi^2 = 13.93$, $p < 0.01$; B4000 $\chi^2 = 11.54$, $p < 0.01$; VB1750 $\chi^2 = 17.35$, $p < 0.01$; VB4000 $\chi^2 = 14.42$, $p < 0.01$; VM: $\chi^2 = 12.03$, $p < 0.01$).

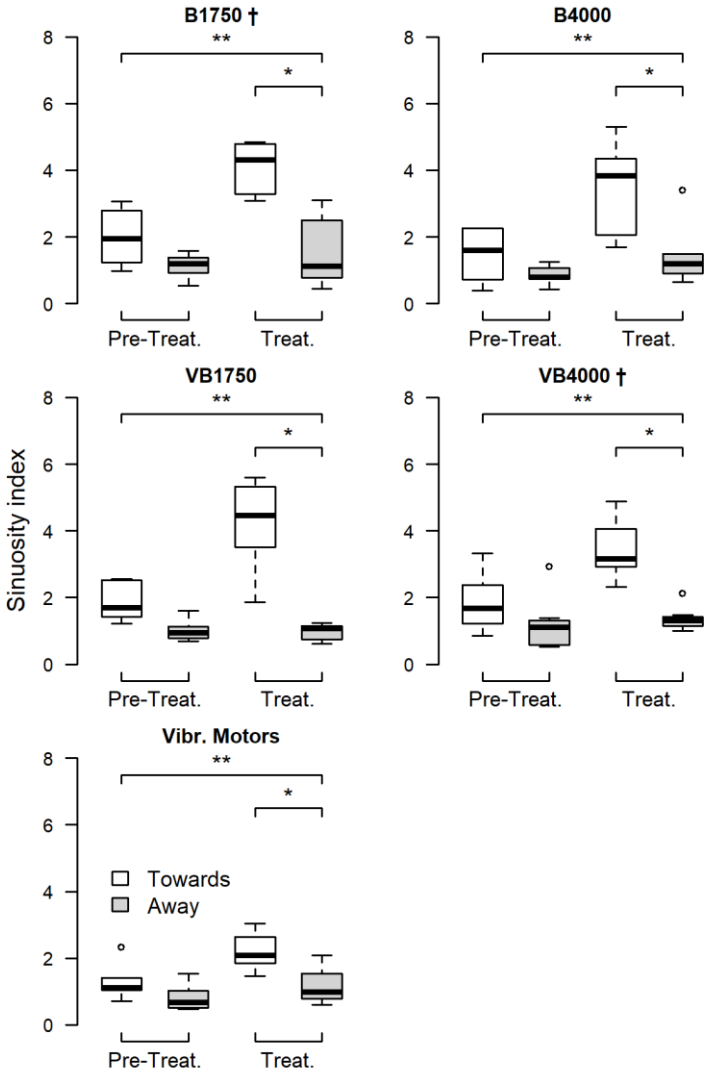

FIG. 8. - The median, interquartile range and minimum/maximum whiskers of the mean sinuosity indices per trial for *Passes* during Experiment 2 (6 L min^{-1} bubble curtain). Pairs with a significant difference are denoted by an asterisk. Resonant treatments are marked by a dagger. B = standard injection, VB = vibrated injection, VM = vibrating motors, and numbers refer to frequency of the sound field.

Distance from the bubble curtain was the most important explanatory variable in the minimum adequate model of *Swimming velocity* for successful passage approaches (Table II), explaining 15.5% of residual deviance. *Swimming velocity* was also correlated with swimming direction, the hydrodynamic gradient, and treatment. For fish rejecting passage, the distance from the bubble curtain, sound pressure gradient, hydrodynamic gradient, and treatment were significant

predictors. Models obtained for the difference angle data explained comparatively lower percentages of deviance in comparison with the swimming velocity models. Distance from the curtain ($p < 0.01$), and swimming direction ($p < 0.01$) explained 9.5% of the variation for passage data, whereas rejection was influenced by distance from the curtain ($p < 0.01$), and PD gradient ($p < 0.01$), which explained 8.5% of deviance.

Experiment 3: influence of visual cues on fish response to an insonified bubble curtain

Under conditions of daylight, the *Number of passes* were lower when a bubble curtain insonified by a 1000 Hz signal was active compared to the controls ($F = 4.97$, $p = 0.01$, p-adj = 0.01). Both treatments were more effective at night than during the day, resulting in lower *Passage efficiencies* ($\chi^2 = 31.93$, $p < 0.01$), with adjusted p-values of 0.048 and < 0.01 for standard and vibrated injection, respectively. The vibrating motors treatment had no effect on either the *Number of passes* or *Passage efficiency*.

For carp that passed the bubble curtain, the approach trajectory was invariably more sinuous than when swimming away from the curtain having passed ($\chi^2 = 64.05$, $p < 0.01$). *Sinuosity* was influenced by treatment and time of day (Table III). During daylight, fish exhibited more sinuous swimming trajectories during the test than the pre- and post-treatment periods for both the standard and vibrating injection treatments (*standard injection:* $\chi^2 = 19.30$, $p < 0.01$; *vibrated injection:* $\chi^2 = 16.59$, $p < 0.01$), while there was no influence on sinuosity when only the vibrating motors were operating ($\chi^2 = 9.28$, $p = 0.098$). At night, *sinuosity* was higher during the test for all three treatments compared with the pre- and post-treatment control periods (*standard injection:* $\chi^2 = 27.29$, $p < 0.01$; *vibrated injection:* $\chi^2 = 22.96$, $p < 0.01$; *vibrating motors:* $\chi^2 = 12.74$, $p = 0.03$). *Sinuosity* differed between treatments depending on whether it was day or night (*Day*: $\chi^2 = 6.13$, p-value = 0.046; *Night:* $\chi^2 = 8.22$, $p = 0.02$).

530 *Sinuosity* was higher during the day only for the vibrated injection treatment (p = 0.04), whereas
531 at night it was higher for both bubble treatments compared to the vibrating motors alone (p =
532 0.01 for both).

533 TABLE II – Results of modelled effects of the stimuli generated by an insonified bubble curtain
534 on fish swimming velocity (Experiment 2). The deviance explained relative to null (%),
535 estimated degrees of freedom (edf) and significance (p-value) of the terms in the minimum
536 adequate model fitted to swimming velocity are listed. Brackets indicate smoothed terms.

Dataset	Model terms	Deviance explained relative to null (%)	edf	p value
Swimming velocity (Passage)	Treatment + Direction + s(Distance from bubble curtain)	21.5 (minimum adequate model)		
	s(Distance from bubble curtain)	16.9	8.27	<0.01
	Direction	4.2	-	<0.01
	Treatment	0.4	-	<0.01
Swimming velocity (Rejection)	Treatment + HydroTreatment + s(Distance from bubble curtain) + s(SD Flow) + s(SPL) + s(PD)	17.6 (minimum adequate model)		
	s(Distance from bubble curtain)	9.47	8.95	<0.01
	s(PD)	5.72	6.91	<0.01
	HydroTreatment	1.41	-	<0.01
	Treatment	0.4	-	<0.01
	s(SD Flow)	0.5	3.8	<0.01
	s(SPL)	0.1	1.01	0.023

537

Bubble curtains did not influence the trajectories of fish under the illuminated condition as they rejected it (Fig. 9). The *Angular dispersion*, r, depended on distance from the bubble curtain, time of day, direction and phase. Using these parameters, the model explained 34% of the deviance. Trajectories were more sinuous during the test compared to the pre/post-treatment controls ($p < 0.01$), and during the vibrated injection treatment ($p = 0.01$).

Swimming velocity was dependent on distance from the bubble curtain, experimental phase, treatment, and time of day, with the model explaining 27.4% of the deviance when approaching the bubble curtain, and 28.4% when swimming away. In both cases, *Swimming velocity* was lower at night ($p < 0.01$), and during the treatment phase compared to the rest of the trial ($p < 0.01$). When approaching the bubble curtain, *Swimming velocity* was lower closer to it ($p < 0.01$) for both bubble treatments compared to the vibrating motors only ($p < 0.01$). When swimming away, velocities were higher farther away from the bubbler ($p < 0.01$), and highest for vibrated injection ($p < 0.01$).

TABLE III – Results obtained for Experiment 3, indicating the influence of an insonified bubble curtain on the sinuosity of fish swimming trajectories under conditions of darkness and illumination. Trajectories were more sinuous for fish swimming towards the bubble curtain during the treatment phase, and at night.

Time	Treatment	Experimental Phase		
		Pre-Treatment	Treatment	Post-Treatment
Day	*Towards bubble curtain*			
	Standard injection	1.08 ± 0.61	**2.34 ± 0.77[a]**	1.23 ± 0.54
	Vibrated injection	1.00 ± 0.63	**3.12 ± 0.80[a]**	1.18 ± 0.55
	Motors	1.14 ± 0.63	1.62 ± 1.03	1.48 ± 1.13

	Away from bubble curtain			
	Standard injection	0.78 ± 0.66	1.28 ± 1.40	0.72 ± 0.80
	Vibrated injection	0.75 ± 0.34	0.94 ± 1.27	0.72 ± 0.37
	Motors	0.58 ± 0.15	0.99 ± 0.38	1.00 ± 0.40
	Towards bubble curtain			
	Standard injection	3.71 ± 1.62	**5.79 ± 2.30[a]**	3.40 ± 1.62
	Vibrated injection	3.18 ± 1.66	**4.63 ± 1.95[a]**	3.89 ± 2.28
	Motors	2.24 ± 1.05	**2.27 ± 1.37[b]**	2.25 ± 1.35
Night	*Away from bubble curtain*			
	Standard injection	1.71 ± 0.44	1.05 ± 0.91	1.42 ± 0.81
	Vibrated injection	1.49 ± 1.09	0.86 ± 0.50	1.70 ± 1.30
	Motors	1.23 ± 0.57	1.05 ± 0.60	1.45 ± 1.28

[a] significant at the 0.01 level
[b] significant at the 0.05 level
values in Bold = significance between treatment and pre/post-treatments

IV DISCUSSION

The novelty of this study relates to three main elements; it is the first to: (1) investigate carp reactions to a low air flow bubble curtain, (2) compare the effectiveness of resonant versus non-resonant insonified bubble curtains to deter passage, determining the stimuli responsible for eliciting deterrence, and (3) consider the effect of visual cues in relation to acoustic and hydrodynamic stimuli generated by the bubble curtain by conducting trials under conditions of illumination and darkness. This study also implemented the first flume deployment of a method

to control bubble size using the same orifices and gas flow, by considering bubble coalescence (Leighton *et al.*, 2012). To accomplish this in a small test tank, the air flow was much lower than what would be used in the field, so the fish responses were expected to be small. However in principle the system could readily be scaled up for field-scale facilities.

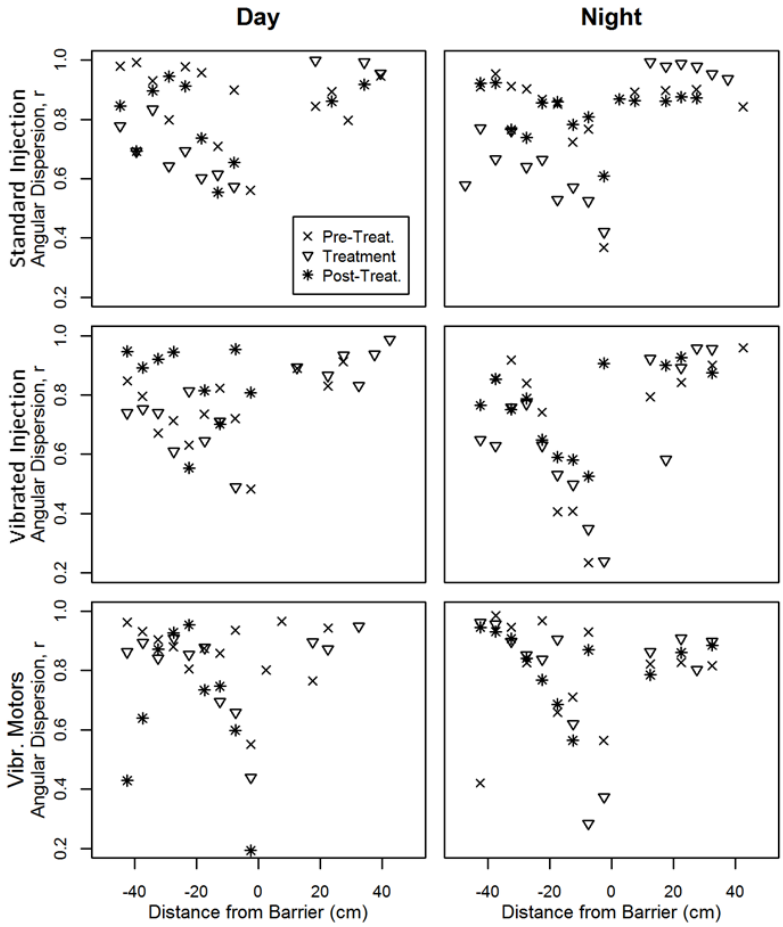

FIG. 9. – Scatterplots of *Angular dispersion* for rejected attempts from Experiment 3 (10 L min^{-1} bubble curtain). Values closer to 1.0 indicate greater directionality. Negative and positive x-axis values indicate motion towards and away from the bubble curtain, respectively.

Our findings show that a bubble curtain with a gas flux of 30 L min^{-1} m^{-1} can be sufficient to reduce passage in carp, deflecting them towards the flume wall. While this experiment was considered as a logical starting point for a series of subsequent experiments, it suggests that bubbles can moderately reduce passage even at low air flows. It also supports

prior findings (Bibko *et al.*, 1974) that fish can detect and make use of gaps in a behavioural barrier using mechanosensory cues in the absence of light.

Resonant insonified bubble curtains reduced passage in carp relatively more than non-resonant bubble curtains. A bubble population that contains more bubbles in resonance with the driving sound field will extract more energy from that field compared with a population that contains less resonant bubbles. We postulate that the more abrupt changes (i.e. the ones marked by a dagger in Figure 4) in the acoustic stimuli due to the presence of a resonant bubble population were more likely to initiate avoidance in carp. Movement of carp away from an insonified bubble curtain appears to have been strongly influenced by the gradients of both particle displacement (ΔPD) and the standard deviation of the flow (ΔSD flow), and these findings appear to support the observations of others. A previous study carried out with an acoustic bubble curtain (720 L min^{-1}, or 180 L min^{-1} m^{-1} of bubble curtain) argued that deterrence is likely caused by acoustic particle motion in the near field of the bubble curtain (Zielinski & Sorensen, 2016). This conclusion was reached by observing that carp rejected passage within 25 cm of the bubble curtain, which coincided with the region of maximum particle acceleration, whereas hydrodynamic forces generated by the bubbles extended from 50 – 100 cm away from it (Zielinski & Sorensen, 2016). In this study hydrodynamic forces decreased rapidly beyond a distance of 25 cm away from the bubble curtain, whereas the higher air flows used to create the bubble curtain in the previous study likely explain their larger hydrodynamic signatures. In our case, rejection responses were likely elicited by multimodal cues; close overlap between the PD and SD flow fields may have enabled them to reinforce one another presenting fish with two sharp gradients in the same region.

In the presence of daylight, insonified bubble curtains reduced passage in carp relatively less. Although course-scale efficiencies of bubble curtains have been known to vary between daylight and night (Welton *et al.*, 2002; Leander *et al.*, 2021), our findings quantified this

behaviourally. In all three experiments, when encountering a bubble curtain in darkness, carp tended to engage in exploratory behaviour, and repeatedly swam along the front of or held position facing it, prior to a pass or rejection. Carp also reduced their swimming speed, and the degree to which this happened, as well as the distance at which reductions were observed was dependent on treatment type. It is likely that non-resonant treatments were better at reducing swimming speeds because the acoustic stimuli could be detected farther away. In daylight, however, these behaviours became less pronounced, noticeable from the higher passage efficiencies, higher swimming speeds, and a decrease in the sinuosity index. While this supports Welton *et al's* (2002) conclusions, Leander *et al.,* (2021) found that bubble curtains alone were more effective at guiding salmon smolts into a fishway during the day. This indicates that in the absence of other sensory cues such as a sound field, visual detection of the bubble curtain is important for eliciting deterrence (Leander *et al.,* 2021). Earlier work suggests that fishes are highly dependent on the mechanosensory system in darkness, but when available, visual cues may be given more importance than hydrodynamic and acoustic signals (Rowe, 1999; Vowles *et al.,* 2014). This could explain our video footage observations in Experiment 3, where fish swam through gaps in the bubble wall during the day, caused by needles moving out of alignment. Although this observation was qualitative, similar conclusions were drawn for Atlantic salmon smolts, which during the day appear to detect gaps in a bubble curtain that occur due to deposition of silt on the perforated pipe, thus reducing the efficiency of the bubble curtain (Welton *et al.,* 2002). Care should be taken when extrapolating these results more generally given that carp behaviour changes with season (Bajer *et al.* 2010), time-of-day (Benito *et al,.* 2015), and temperature (Rome *et al.,* 1985).

Vibrating motors had a deterrent effect on fish behaviour in Experiment 2, reducing passage count by 30% of a pre-test control, but not in Experiment 3. This was likely due to the louder broadband sound levels generated by the motors at 3V (123 dB re 1 μPa) versus 2.2V

628 (106 dB re 1 μPa). Although the deterrent effect of the VM treatment can be compared with
629 the bubble treatments, it cannot be directly subtracted to obtain the deterrent effect of the
630 bubbles minus the motors. This is because the bubble curtains attenuated a substantial portion
631 of the sound generated by the motors below 2 kHz (See supplementary material at [URL will
632 be inserted by AIP] for recorded acoustic spectra).

633 For Experiments 2 and 3, the range of σ_e^{90} was narrow for every insonified bubble
634 curtain tested, and narrowest for the resonant set-ups. This implies that if past or future bubble
635 curtain deployments injected a suboptimal bubble size; either by injecting a very wide range
636 such that much of the gas pumped in does not contribute to the acoustical effect, or by
637 generating a bubble cloud that does not contain resonant bubbles, they could be highly
638 inefficient. By altering the size of bubble generated, a large-scale deployment could change
639 from not being cost-effective, to being practicable, efficient and affordable.

640 It is important to draw attention to certain historical pitfalls when conducting
641 experiments with underwater bubbles. The use of bubble curtains to contain sound fields
642 through backscattering or attenuation dates back to 1948 (Loye & Arndt, 1948). Evaluations
643 of bubble curtains used as behavioural deterrents for fish were also carried out at a number of
644 sites on the Great Lakes in the 1970's (Hocutt, 1980), although many of these studies were grey
645 literature reports, and lacked methodological details or in-depth categorisation of the stimuli
646 used (Popper & Carlson, 1998). The description of the apparatus showed no obvious capability
647 to control bubble size or optimize it for the sound field in question. Results were mixed and
648 research into their use dropped. Recently, however, the interest in bubble curtains has been
649 renewed due to the need to develop cost-effective and easily deployable barriers to prevent the
650 spread of invasive carp in North America (Kelly *et al.*, 2011) and Australia (Koehn *et al.*,
651 2000), and also to protect them in their native range (Xu *et al.*, 1992; Chen *et al.*, 2004). Despite
652 the historical body of work on bubble curtains, the push towards specifying and measuring the

653 stimuli they generate is a fairly recent one (Dawson *et al.*, 2006; Zielinski & Sorensen, 2016;
654 Dennis *et al.*, 2019). It is essential that this continues, and for the behavioural scientist to be
655 able to carry out valid research and properly compare and interpret the results of others. The
656 historical body of work has relied on a 'brute force' approach, where the only driver to improve
657 deterrence has been to pump more air, or add additional stimuli, which eventually becomes
658 unfeasible if demands for scale-up increase. By understanding bubble formation, and the
659 interaction of the bubble and the sound field, powerful gains towards scale-up can be made for
660 less effort (e.g. encapsulating stationary bubbles (Lee *et al.*, 2016); or exploiting the resonance,
661 as discussed here).

662 When using bubbles to create a multimodal stimulus (e.g. with sound) great care should
663 be taken to consider what determines the size of a bubble, and how this may affect its properties
664 and the replicability of the study. For a given nozzle size, there is a bubble of maximum volume,
665 and its size depends on: (1) the rate of air flow to the bubble, and (2) whether the system is
666 operated in a pressure-controlled or volume-controlled mode (Longuet-Higgins *et al.*, 1991;
667 Clift *et al.*, 1978). When introducing air underwater, as gas flow is increased, rising bubbles
668 come into contact with one another and coalesce to form larger bubbles. Higher flow rates (e.g.
669 30 mL s^{-1} per nozzle) result in a wide range of bubble sizes growing at the orifice or generated
670 by the fragmentation of existing bubbles (Leighton *et al.*, 1991). Since detachment and
671 fragmentation occur unpredictably, using the size of the orifice to measure the bubble size used
672 in an experiment is unreliable.

673 Our study used the tactic of generating bubble curtains using the same apertures and
674 gas fluxes, but activated with different levels of needle vibration, to determine how fish react
675 to bubble curtains. Following Leighton *et al.*, (2012, with video at
676 www.isvr.soton.ac.uk/fdag/PIPE_DEMO/index.htm) needles that would normally generate
677 bubbles that are ineffective at absorbing sound would, when vibrated, produce a cloud of much

678 smaller bubbles because they did not coalesce at the nozzle (Leighton *et al.*, 1991). Being closer
679 to resonance with the acoustic field, these smaller bubbles attenuated sound better, even though
680 the gas flow rate into the needle was unchanged. This demonstrates that simply stating the gas
681 flow rate and aperture size is not sufficient to characterise an acoustically-active bubble curtain,
682 because the bubble size distribution also has to be known. Knowing the size composition of
683 the bubble population, gas flow rate, and the gas pressure in addition to mapping the fields for
684 the various stimuli generated should be considered a starting point for future experiments
685 involving bubbles and sound. Determining, σ_e^{90}, the size fractions responsible for 90% of the
686 extinction of the energy from an incident wave could prove a useful tool to determine the most
687 effective range of frequencies to use for a given bubble population.

688 While 4000 Hz is not within the most sensitive range of carp hearing (e.g. Vetter *et al.*,
689 2018), the approach taken here was to match the sound frequencies to the bubbles generated.
690 In line with carp audiograms, in Experiment 2 the 4000 Hz set-ups were relatively less effective
691 than their respective 1750 Hz treatments. However, carp also reacted to the particle motion or
692 hydrodynamic field for which behavioural audiograms do not currently exist (Popper &
693 Hawkins, 2019). Furthermore, the ability of a fish to detect a sound may not necessarily evoke
694 a response (Putland & Mensinger, 2019; Leighton *et al.*, 2020).

695 Much scope remains for future research and a logical next step would be to maximise
696 deterrence. Using slightly higher air flows (e.g. 10 – 20 L min^{-1} m^{-1}) the deterrent effect of
697 resonant bubble curtains insonified by: (1) a single tone versus, (2) multiple tones, and (3)
698 broadband signals, each selected specifically to drive one or more bubble size ranges to
699 resonance, could be compared. The influence of group effects (e.g. Currie *et al.*, 2020) and
700 long-term habituation could also be considered (Putland & Mensinger, 2019). We echo earlier
701 calls (e.g. Deleau *et al.*, 2019) that such technologies should not be used as an absolute barrier,
702 but incrementally improved to deflect, or redirect fishes; e.g towards fish passes where even

703 moderate improvements in passage rates could help conserve sensitive species. To avoid
704 habituation such deterrents are best used in situations where fish will be in contact with the
705 stimulus for a brief period of time such as during a migration, or in tidal areas (Turnpenny &
706 O'Keefe, 2005, Zielinski & Sorensen, 2016).

707 V CONCLUSIONS

708 This study used injection nozzles and vibrating motors to generate populations of underwater
709 bubbles of different size and composition while using the same air flow. These were insonified
710 by sound fields of different frequencies to test the effectiveness of resonant versus non-resonant
711 insonified bubble curtains as deterrents for fish passage, and in the absence or presence of
712 visual cues. Results show that bubble curtains in resonance with a sound field show relatively
713 improved deterrence, and that passage rejection in common carp is likely mediated by
714 multimodal cues. The presence of visual cues increased passage efficiency and swimming
715 velocity, and fish followed less sinuous trajectories compared to the same conditions in the
716 dark. This indicates, at least under the experimental conditions described here, that visual cues
717 are important for carp.

718 When working with bubble curtains, due consideration should be given to what
719 influences the size of a bubble, and how this affects the way a bubble cloud interacts with an
720 incident sound field. Care should be taken to ensure replicability and better control over the
721 stimuli generated through detailed categorisation.

722 VI ACKNOWLEDGMENTS

723 The lead author was funded by an EPSRC Doctoral Training Centre grant. We thank A.
724 Holgate, Dr. T. Tsuzaki, and K. Scammell for assistance with designing and constructing the
725 bubble generator, and experimental set-up; S. Haściłowicz, and J. Miles for their coding inputs;
726 Dr Kyungmin Baik for helpful discussions on the scattering cross-sections; and members of

727 the International Centre for Ecohydraulics Research (ICER), the Centre for Doctoral Training
728 in Sustainable Infrastructure Systems (CDT-SIS), and the Institute for Sound and Vibration
729 Research (ISVR) for experimental cover, and various discussions, suggestions and constructive
730 comments provided throughout.

731

See supplementary material at [URL will be inserted by AIP] for [give brief description of material]

VII REFERENCES

Ainslie, M. A., and Leighton, T. G. (**2009**). "Near resonant bubble acoustic cross-section corrections, including examples from oceanography, volcanology, and biomedical ultrasound", J. Acoust. Soc. Am. **126**(5), 2163-2175.

Ainslie, M. A., and Leighton, T. G. (**2011**). "Review of scattering and extinction cross-sections, damping factors, and resonance frequencies of a spherical gas bubble," J. Ac. Soc. Am. **130**(5), 3184–3208.

Amaral, S. V., Winchell, F. C., McMahon, B J., and Dixon, D.A. (**2003**). "Evaluation of angled bar racks and louvers for guiding silver phase American eels," in: Management and Protection of Catadromous Eels, edited by Dixon D. A., (American Fisheries Society, Symposium 33, Bethesda, MD, 2003), pp. 367-376.

Andreeva, I. B. (**1964**). "Scattering of sound by air bladders of fish in deep sound-scattering ocean layers," Sov. Phys. Acoust. **10**, 17–20.

Baik, K. (**2013**). "Comment on 'Resonant acoustic scattering by swimbladder-bearing fish' [J. Acoust. Soc. Am. 64, 571–580 (1978)] (L)," J. Acoust. Soc. Am. **133** (1), 5-8.

Bajer, P. G., Lim, H., Travaline, M. J., Miller, B. D., and Sorensen, P. W. (**2010**). "Cognitive aspects of food searching behavior in free-ranging wild Common Carp," Environ. Biol. Fish. **88**, 295–300.

Batschelet, E. (**1981**). "Circular Statistics in Biology" Academic Press, London.

Benhamou, S. (**2004**). "How to reliably estimate the tortuosity of an animal's path: straightness, sinuosity, or fractal dimension?" J. Theor. Biol. **229**, 209-220.

Benito, J., Benejam L., Zamora, L., Garcia-Berthou, E. (**2015**). "Diel Cycle and Effects of Water Flow on Activity and Use of Depth by Common Carp," Trans. Am. Fish. Soc. **144**, 491-501.

Bibko, P. N., Wirtenan, L. and Kueser, P. E. (**1974**). "Preliminary studies on the effects of air bubbles and intense illumination on the swimming behavior of the striped bass (*Morone saxatilus*) and the

gizzard shad (*Dorosoma cepedianum*)," in: Entrainment and Intake Screening. Proc. 2nd Entrain. Intake Screen Workshop, edited by L.D. Jensen (John Hopkins University, Baltimore, MD, 1974) pp. 293-304.

Bovet, P., and Benhamou, S. (**1998**). "Spatial analysis of animals' movements using a correlated random walk model," J. Theor. Biol. **131**, 419-433.

Budaev, S. V., Zworykin, D. D. (**2002**). "Individuality in fish behavior: ecology and comparative psychology," J. Ichthy. **42** (2), 189–195.

Burnham, K. P. and Anderson, D. R. (**2002**). Model Selection and Multimodel Inference. A Practical Information-Theoretical Approach. Springer-Verlag, New York.

Brett, J. R., and MacKinnon, K. D. (**1953**) "Preliminary experiments using lights and bubbles to deflect migrating young spring salmon," J. Fish. Res. Bd. Can. **10**(8), 548-559 (1953).

Brevik, I. and Kristiansen Ø. (**2002**). "The flow in and around air-bubble plumes," Int. J. Multiph. Flow. **28**, 617–634.

Calles, O., Olsson, I. C., Comoglio, C., Kemp, P. S., Blunden, L., Schmitz, M., and Greenberg, L. A. (**2010**). "Size-dependent mortality of migratory silver eels at a hydropower plant, and implications for escapement to the sea," Freshw. Biol. **55**, 2167–2180.

Chen, D., Duan, X., Liu, S., and Shi, W. (**2004**). "Q9 Status and management of fishery resources of the Yangtze river". In: Welcomme, R., Petr, T. (Eds.), Proceedings of the Second International Symposium on the Management of Large Rivers for Fisheries, vol. I., (RAP Publication 2004/16, FAO Regional Office for Asia and the Pacific, Bangkok, 2004), pp. 173–182.

Clift, R., Grace, J. R., and Weber, W. E. (**1978**). "Bubbles, Drops and Particles," Academic Press, London.

Currie, H. A. L., White, P. R., Leighton, T. G., and Kemp, P. S. (**2020**). "Group behavior and tolerance of Eurasian minnow (*Phoxinus phoxinus*) in response to tones of differing pulse repetition rate," J. Acoust. Soc. Am. **147**(3), 1709-1718.

781 Dawson, H. A., Reinhardt, U. G., and Savino, J. F. (**2006**) "Use of electric or bubble barrier to limit the
782 movement of Eurasion Ruffe (*Gymnocephalus cernuus*)," J. Great Lakes Res. **32**, 40–49.

783 Deleau, M. J. C., White, P. R., Peirson, G., Leighton, T. G., and Kemp P. S. (**2019**). "Use of acoustics
784 to enhance the efficiency of physical screens designed to protect downstream moving European eel
785 (*Anguilla anguilla*)," Fish. Manag. Ecol. **27**(1), 1-9.

786 Deleau, M. J. C., White, P. R., Peirson, G., Leighton, T. G., and Kemp P. S. **(2020**) "The response of
787 anguilliform fish to underwater sound under an experimental setting". River Res. Applic. **36** (3), 441-
788 451.

789 Dennis, C. E., Zielinski, D. P., and Sorensen, P. W. (**2019**). "A complex sound coupled with an air
790 curtain blocks invasive carp passage without habituation in a laboratory flume," Biol. Inv. **21**, 2837–
791 2855.

792 Enders, E. C., Gessel, M. H., and Williams, J. G. (**2009**). "Development of successful fish passage
793 structures for downstream migrants requires knowledge of their behavioural response to accelerating
794 flow" Can. J. Fish. Aquat. Sci. **66**, 2109–2117.

795 Flammang, M. K., Weber, M. J., and Thul, M. D. (**2014**). "Laboratory evaluation of a bioacoustic
796 bubble strobe light barrier for reducing Walleye escapement," N. Am. J. Fish. Manage. **34**, 1047–1054.

797 Goodwin, R. A., Politano, M., Garvin, J. W., Nestler, J. M., Haye, D., Anderson, J. J., Weber, L.,
798 Dimperio, E., Smith, D. L., and Timko, M. (**2014**). "Fish navigation of large dams emerges from their
799 modulation of flow field experience," PNAS. **111** (14), 5277–5282.

800 Hickling, R. and Wei, W. (**1995**). "Use of pitch-azimuth plots in determining the direction of a noise
801 source in water with a vector sound-intensity probe," J. Acoust. Soc. Am. **97** (2), 856-886.

802 Hocutt, C. H. (**1980**). "Behavioral barriers and guidance systems," in: Power Plants: Effects on Fish
803 and Shellfish Behaviour, edited by Hocutt, C. H., Stauffer, J. R. Jr, Edinger, J. E., Hall, L. W. Jr, and
804 Morgan, R. P. II (New York: Academic Press), pp. 183–205.

805 Huntingford, F. A., Andrew, G., Mackenzie, S., Morera, D., Coyle, S. M., and Pilarczk Kadri S. (**2002**).
806 "Coping strategies in a strongly schooling fish, the Common Carp *Cyprinus carpio*," J. Fish Biol. **76**,
807 1576–1591.

808 Inglis, M. L., McCoy, G. L., and Robson, M. (**2016**). "Testing the effectiveness of fish screens for
809 hydropower intakes," (Environment Agency, Bristol).

810 IOE Group (**1994**). "The development of a non-physical fish fence using combined infrasonic and
811 electric fields – fish behavioural trials," Report to the EC under the 3rd Framework Agriculture and
812 Agro-Industries (AIR) Programme, Project Ref. AIR 10113.

813 Jansen, H. M., Winter, H. V., Bruijs, M. C. M., and Polman, J. G. (**2007**). "Just go with the flow? Route
814 selection and mortality during downstream migration of silver eels in relation to river discharge," ICES
815 J. Mar. Sci. **64**, 1437–1443.

816 Johnson, N. S., Yun, S. S., Thompson, H. T., Brant, C. O., and Li, W. (**2009**) "A synthesized pheromone
817 induces upstream movement in female sea lamprey and summons them into traps," Proc. Natl. Acad.
818 Sci. U.S.A. **106** (4), 1021–1026.

819 Katopodis, C., and Williams, J. G. (**2012**). "The development of fish passage research in a historical
820 context," Ecol. Eng. **48**, 8-18.

821 Kelly, A. M., Engle, C. R., Armstrong, M. L., Freeze, M., and Mitchell, A. J. (**2011**). "History of 19
822 introductions and governmental involvement in promoting the use of grass, silver, and bighead carps.
823 Invasive Asian Carps in North America", American Fisheries Society Special Symposium. **74**, 163-
824 174.

825 Kemp, P. S., Anderson, J. J., and Vowles, A. S. (**2012**). "Quantifying behaviour of migratory fish:
826 Application of signal detection theory to fisheries engineering," Ecol. Eng. **41**, 22–31.

827 Kemp, P. S., Gessel, M. H., and Williams, J. G. (**2005**). "Seaward migrating subyearling Chinook
828 salmon avoid overhead cover," J. Fish Biol. **67**, 1381–1391.

829 Koehn, J., Brumley, A., & Gehrke, P. (**2000**). "Managing the Impacts of Carp," Bureau of Rural
830 Sciences (Department of Agriculture, Fisheries and Forestry – Australia), Canberra.

831 Kuznetsov, Y. A. (**1971**). "The behavior of fish in the zone affected by a curtain of air bubbles," in:
832 Fish Behavior and Fishing Techniques, edited by A.P. Alekeseev (Nat. Mar. Fish. Serv., NOAA, Nat.
833 Tech. Info. Serv., Translation No. TT 71-50010, 1971) pp. 103-110.

834 Leander, J., Klaminder, J., Hellström, G., Jonsson, M. (**2021**). "Bubble barriers to guide downstream
835 migrating Atlantic salmon (Salmo salar): An evaluation using acoustic telemetry," Ecol. Eng. **160**,
836 106141.

837 Lee, K. M., Wochner, M. S., Wilson, P. S. (**2016**). "Passive Underwater Noise Attenuation Using Large
838 Encapsulated Air Bubbles". In: Popper, A., Hawkins, A. (Eds.), The Effects of Noise on Aquatic Life
839 II. Advances in Experimental Medicine and Biology, vol 875. Springer, New York, pp. 607-614.

840 Leighton, T. G. (**1994**). "The Acoustic Bubble", Academic Press, London.

841 Leighton, T. G., Baik, K., and Jiang, J. (**2020**). "Educational demonstration of sound attenuation in a
842 water-filled pipe," www.isvr.soton.ac.uk/fdag/PIPE_DEMO/index.htm (Last viewed September 25,
843 2020).

844 Leighton, T. G., Currie, H. A. L., Holgate, A., Dolder, C. N., Lloyd Jones, S., White, P. R., and Kemp,
845 P. S. (**2020**). "Analogies in contextualizing human response to airborne ultrasound and fish response to
846 acoustic noise and deterrents," Proceedings of Meetings on Acoustics **37**, 010014.

847 Leighton, T. G., Fagan, K. J., and Field, J. E. (**1991**). "Acoustic and photographic studies of injected
848 bubbles," Eur. J. Phys. 77–85.

849 Leighton, T. G., Jiang, J., and Baik, K. (**2012**). "Demonstration comparing sound wave attenuation
850 inside pipes containing bubbly water and water droplet fog," J. Acoust. Soc. Am. **131**(3 pt 2), 2413-
851 2421.

852 Leighton, T. G., Ramble, D. G., Phelps, A. D., Morfey, C. L., and Harris, P. P. (**1998**). "Acoustic
853 detection of gas bubbles in a pipe," Acta Acustica. **84**, 801-814.

Lewis, W. M., Heidinger, R., and Konikoff, M. (**1968**). “Loss of fishes over the drop box spillway of a lake,” Trans. Am. Fish. Soc. **97**, 492–494.

Li, J., Roche, B., Bull, J., White, P. R., Leighton, T., Provenzano, G., Dewar, M., and Henstock, T. (**2020**). “Broadband acoustic inversion for gas flux quantification - application to a methane plume at Scanner Pockmark, central North Sea”. J. Geophys. Res. Oc. **125**(9), e2020JC016360.

Longuet-Higgins, M. S., Kerman, B. R., and Lunde, K. (**1991**). “The release of air bubbles from an underwater nozzle,” J. Fluid. Mech. **230**, 365-390.

Lowe, R. H. (**1952**). “The influence of light and other factors on the seaward migration of the silver eel (*Anguilla anguilla* L.),” J. Anim. Ecol. **21**, 275–309.

Loye, D. P., Arndt, W. F. (**1948**). “An acoustic screen for making underwater noise reduction tests in Pearl Harbor,” J. Acoust. Soc. Am. **20**, 224.

Maes, J., Turnpenny, A. W. H., Lambert, D. R., Nedwell, J. R., Parmentier, A., and Ollevier, F. (**2004**). “Field evaluation of a sound system to reduce estuarine fish intake rates at a power plant cooling water inlet,” J. Fish Biol. **64**, 938–946.

McIninch, S. P., and Hocutt, C. H. (**1987**). “Effects of turbidity on estuarine fish response to strobe lights,” J. Appl. Icthyol. **3,** 97–105.

Minnaert, M. (**1993**). “On musical air-bubbles and the sound of running water,” Philos. Mag. **16**, 235-248.

Moser, M. L., Jackson, A. D., Lucas, M. C., and Mueller, R. P. (**2014**). "Behavior and potential threats to survival of migrating lamprey ammocetes and macrophthalmia," Rev. Fish Biol. Fish. **25**, 103-116.

Noatch, M. R., and Suski, C. D. (**2012**). “Non-physical barriers to deter fish movements,” Environ. Rev. **20**, 1-12.

Patrick, P. H., Christie, A. E., Sager, D., Hocutt, C., and Stauffer J. Jr. (**1985**). “Responses of fish to a strobe light/air-bubble barrier,” Fish. Res. **3**, 157–172.

878 Piper, A. T., White, P. R., Wright R. M., Leighton T. G., and Kemp P. S. (**2019**). "Response of seaward-
879 migrating European eel (*Anguilla anguilla*) to an infrasound deterrent," Ecol. Eng. **127**, 480-486.

880 Popper, A. N., and Carlson, T. J. (**1998**). "Application of Sound and Other Stimuli to Control Fish
881 Behavior," Trans. Am. Fish. Soc. **127** (5), 673–707.

882 Popper, A. N., and Hawkins, A. D. (**2019**). "An overview of fish bioacoustics and the impacts of
883 anthropogenic sounds on fishes," Fish Biol. **94** (5), 692-713.

884 Putland, R. L., and Mensinger, A. F. (**2019**)."Acoustic deterrents to manage fish populations," Rev.
885 Fish Biol. Fisheries **29**, 789-807.

886 Rome, L.C., Loughna, P.T., Goldspink, G. (**1985**). "Temperature Acclimation: Improved Sustained
887 Swimming Performance in Carp at Low Temperatures," Science **228** (4696), 194-196.

888 Rowe, C. (**1999**). "Receiver psychology and the evolution of multicomponent signals," Anim. Behav.
889 **58**, 921-931.

890 Sager, D. Hocutt, C., and Stauffer J. Jr. (**1987**). "Estuarine fish responses to strobe light,bubble curtains
891 and strobe light/bubble-curtain combinations as influenced bywater flow rate and flash frequencies,"
892 Fish. Res. **5**, 383–399.

893 Sand, O. (**2000**). "Avoidance responses to infrasound in downstream migrating European silver eels,
894 *Anguilla anguilla*," Env. Biol. Fish. **57**, 327–336.

895 Sisler, S. P., and Sorensen, P. W. (**2008**). "Common carp and goldfish discern conspecific identity using
896 chemical cues," Behaviour **145**, 1409-1425.

897 Sloan, J. L., Cordo, E. B., and Mensinger, A. F. (**2013**). "Acoustical conditioning and retention in the
898 common carp (*Cyprinus carpio*)," J. Great Lakes Res. **39**, 507–512.

899 Solomon, D. J. (**1992**). "Diversion and entrapment of fish at water intakes and outfalls," R & D Report
900 No. 1, (National Rivers Authority, Bristol).

Turnpenny, A. W. H., and O'Keefe, N. (**2005**). "Screening for intake and outfalls: a best practice guide," Vol. W6-103/TR. (Environment Agency, Bristol).

Sorensen, P. W., and Stacey, N. E. (**2010**). "Brief review of fish pheromones and discussion of their possible uses in the control of non-indigenous teleost fishes," New Zeal. J. Mar. Fresh. **38**, 399–417.

Stewart, H. A., Wolte, M. H., and Wahl, D. H. (**2014**) "Laboratory investigations on the use of strobe lights and bubble curtains to deter dam escapes of age- 0 Muskellunge," N. Am. J. Fish. Manage. **34**, 571–575.

Taylor, R. M., Pegg, M. A., and Chick, J. H. (**2005**). "Response of Bighead Carp to a bioacoustic behavioural fish guidance system," Fish. Manage. Ecol. **12**, 283–286.

Turnpenny, A. W. H., Struthers, G., and Hanson, K. P. (**1998**). "A UK Guide to Intake Fish-Screening Regulations, Policy and Best Practice". Contractors report to the Energy Technology Support Unit, Harwell, Project No. ETSU H/00052/00/00.

Vetter, B. J., Cupp, A. R., Fredriks, K. T., Gaikowski, M. P., and Mensinger, A. F. (**2015**). Acoustical deterrence of silver carp (*Hypophthalmichthys molitrix*). Biol. Invasions **17**, 3383–3392.

Vetter, B. J., Murchy, K. A., Cupp, A. R., Amberg, J. J. , Gaikowski, M. P., and Mensinger, A. F. (**2017**). "Acoustic deterrence of bighead carp (*Hypophthalmichthys nobilis*) to a broadband sound stimulus," J.Gr. Lakes Res. **43**, 163-171.

Vetter, B. J., Brey, M. K., and Mensinger, A. F. (**2018**). Reexamining the frequency range of hearing in silver (*Hypophthalmichthys molitrix*) and bighead *(H. nobilis*) carp. PLoS ONE **13**(3): e0192561.17Vowles, A. S., Anderson, J. J., Gessel, M. H., Williams, J. H., and Kemp, P. S. (**2014**). "Effects of avoidance behaviour on downstream fish passage through areas of accelerating flow when light and dark," Anim. Behav. **92**, 101-109.

Vowles, A. S., and Kemp, P.S. (**2012**). "Effects of light on the behaviour of brown trout (*Salmo trutta*) encountering accelerating flow: application to downstream fish passage," Ecol. Eng. **47**, 247-253.

925 Wagner, C. M., Stroud, E. M., Meckley, T. D., Kraft, C. (**2011**). "A deathly odor suggests a new
926 sustainable tool for controlling a costly invasive species," Can. J. Fish. Aquat. Sci. **68** (7), 1157–1160.

927 Weston, D. E. (**1967**). "Sound propagation in the presence of bladder fish," in Underwater Acoustics,
928 Proc. 1966 NATO Advanced Study Institute, Copenhagen, edited by Albers, V. M. (Plenum, New
929 York), Vol. II, pp. 55–88.

930 Welton, J. S., Beaumont, W. R. C., and Clarke, R. T. (**2002**). "The efficacy of air, sound and acoustic
931 bubble screens in deflecting Atlantic salmon, *Salmo salar* L., smolts in the River Frome," UK. Fish.
932 Manage. Ecol. **9**, 11–18.

933 Wu, X., Rao, J., and He, B. (**1992**). "The history of the Chinese freshwater fisheries," in: Cultivation of
934 the Chinese Freshwater Fishes, edited by Liu, J., and He, B. (Science Press, Beijing, 1992), pp. 5–29.

935 Zeddies, D. G., Fay, R. R., Alderks, P. W., Shaub, K. S., and Sisneros, J. A. (**2010**). "Sound source
936 localization by the plainfin midshipman fish, *Porichthys notatus*," J. Acoust. Soc. Am. **127**, 3104-3113.

937 Zielinski, D. P., Voller, V. R., Svendsen, J. C., Hondzo, M., Mensinger, A. F., and Sorensen, P. (**2014**).
938 "Laboratory experiments demonstrate that bubble curtains can effectively inhibit movement of common
939 carp," Ecol. Eng. **67**, 95–103.

940 Zielinski, D. P., and Sorensen, P. W. (**2015**). "Field test of a bubble curtain deterrent system for common
941 carp," Fish. Management Eco. **22**, 181-184.

942 Zielinski, D. P., and Sorensen, P.W. (**2016**). "Bubble Curtain Deflection Screen Diverts the Movement
943 of both Asian and Common Carp". N. Am. J. Fish. Manage. **36**, 267–276.

944 Zielinski, D. P., & Sorensen, P. W. (**2017**). "Silver, bighead, and common carp orient to acoustic particle
945 motion when avoiding a complex sound," PLoS One **12**, e0180110.

946

947

948

VIII TABLES

TABLE I. Mean length, weight, and holding tank temperature for common carp used in the three experiments to investigate their response to insonified bubble curtains.

Experiment no.	Date	Mean (±SE) length (mm)	Mean (±SE) weight (mm)	Mean (±SE) tank temp. (ºC)
Experiment 1	July 2017	117.6 (21.8)	25,2 (17.5)	17.9 (0.02)
Experiment 2	July 2018	116.1 (0.7)	23.1 (0.5)	20.7 (0.3)
Experiment 3	Feb 2017	97.6 (0.6)	17.0 (0.4)	5.4 (0.4)

TABLE II – Results obtained for the modelled effects of the stimuli generated by an insonified bubble curtain on fish swimming velocity (Experiment 2). The deviance explained relative to null (%), estimated degrees of freedom (edf) and significance (p value) of the terms in the minimum adequate model fitted to swimming velocity are listed. Brackets indicate smoothed terms.

Dataset	Model terms	Deviance explained relative to null (%)	edf	p value
Swimming velocity (Passage)	Treatment + Direction + s(Distance from bubble curtain)	21.5 (minimum adequate model)		
	s(Distance from bubble curtain)	16.9	8.27	<0.01
	Direction	4.2	-	<0.01
	Treatment	0.4	-	<0.01
Swimming velocity (Rejection)	Treatment + HydroTreatment + s(Distance from bubble curtain) + s(SD Flow) + s(SPL) + s(PD)	17.6 (minimum adequate model)		
	s(Distance from bubble curtain)	9.47	8.95	<0.01
	s(PD)	5.72	6.91	<0.01
	HydroTreatment	1.41	-	<0.01
	Treatment	0.4	-	<0.01
	s(SD Flow)	0.5	3.8	<0.01
	s(SPL)	0.1	1.01	0.023

970 TABLE III – Results obtained for Experiment 3, indicating the effect of visual cues and an
971 insonified bubble curtain on the sinuosity of fish swimming trajectories. Trajectories were more
972 sinuous for fish swimming towards the barrier during the treatment phase, and at night.

Dataset	Model terms	Deviance explained relative to null (%)	edf	p value
Swimming velocity (Passage)	Treatment + Direction + s(Distance from bubble curtain)	21.5 (minimum adequate model)		
	s(Distance from bubble curtain)	16.9	8.27	<0.01
	Direction	4.2	-	<0.01
	Treatment	0.4	-	<0.01
Swimming velocity (Rejection)	Treatment + HydroTreatment + s(Distance from bubble curtain) + s(SD Flow) + s(SPL) + s(PD)	17.6 (minimum adequate model)		
	s(Distance from bubble curtain)	9.47	8.95	<0.01
	s(PD)	5.72	6.91	<0.01
	HydroTreatment	1.41	-	<0.01
	Treatment	0.4	-	<0.01
	s(SD Flow)	0.5	3.8	<0.01
	s(SPL)	0.1	1.01	0.023

973

974 [a] significant at the 0.01 level
975 [b] significant at the 0.05 level
976 values in Bold = significance between treatment and pre/post-treatments
977

978

979

IX FIGURES

FIG. 1 (a) Schematic of the bubble curtain and air supply system used for Experiments 2 and 3 of a study to investigate the response of common carp to insonified bubble curtains in the presence and absence of visual cues. A single needle is shown for simplification, all needles were at same depth. (b) Plan of the experimental set-up used in Experiments 2 and 3. Grey areas indicate section of flume not used in experiment, dark grey blocks indicate mesh barriers. The asterisk indicates the release point for fish at the start of each trial. Set-up was asymmetrical due to presence of a walkway, although no differences in attempts or passage efficiency were found between the smaller and larger side of the set-up.

FIG. 2. – Distribution of bubble diameters (μm) at (a) 6 L min^{-1}, with standard injection (0 V), and vibration at 3 V; and (b) 10 L min^{-1} with standard injection (0 V) and vibration at 2.2 V. When the vibrating motors were activated, the general increase in bubble counts for the same volume gas flux was because the gas was distributed in more, smaller bubbles. Note that the volume of gas in the largest non-vibrating bubble peaks (diameters $>10^{3.5}$ microns for (a) and $>10^{6}$ microns for (b) disappeared when vibration (3 V) was activated, and these peaks contained the bulk of the gas.

FIG. 3. – Modelled extinction cross sections for bubble distributions determined for Experiments 2 and 3: a) an air flow of 6 L min^{-1} insonified at either 1750 Hz or 4000 Hz, with either standard injection or vibration at 3 V, and b) an air flow of 10 L min^{-1} insonified at 1000 Hz with standard injection or vibration at 2.2V. σ_e^{90} represents the range of bubble diameters at which the central 90% of the attenuation occurs. The populations with a higher proportion of bubbles at resonance with the sound field are: 1750 Hz standard injection, 4000 Hz vibrated injection, 1000 Hz standard injection.

FIG. 4. – (Colour online) Acoustic maps at 45 cm depth for: (a) 1750 Hz bubble set-ups; (b) 4000 Hz bubble set-ups. Resonant treatments are marked by a dagger (Experiment 2). B = standard injection, VB = vibrated injection. On this scale the nearest edge of the loudspeaker is at horizontal position -17 cm, and the centre of the speaker at horizontal position -26 cm. Sound maps of the speakers alone were included to illustrate the strong attenuating effect from the bubbles.

FIG. 5. – (Colour online) Particle displacement in the: (a) x y z direction, and (b) maps at 20 cm depth. Resonant treatments are marked with a dagger (Experiment 2). B = standard injection, VB = vibrated injection, VM = vibrating motors, and numbers refer to frequency of the sound field.

FIG. 6. – The median, interquartile range and minimum/maximum whiskers of the *Number of passes* and *Passage efficiency* for all treatments for the 6 L min^{-1} bubble curtain during pre-treatment and test periods. Pairs where a significant difference was determined are denoted by an asterisk. Resonant treatments are marked by a dagger. B = standard injection, VB = vibrated injection, VM = vibrating motors, and numbers refer to frequency of the sound field.

FIG.7. – Scatter plots of rejection counts against gradients (averaged for 10 cm bins) of all three stimuli generated by the bubble curtains.

FIG. 8. - The median, interquartile range and minimum/maximum whiskers of the mean sinuosity indices per trial for *Passes* during Experiment 2 (6 L min^{-1} bubble curtain). Pairs with a significant difference are denoted by an asterisk. Resonant treatments are marked by a dagger. B = standard injection, VB = vibrated injection, VM = vibrating motors, and numbers refer to frequency of the sound field.

1025 FIG. 9. – Scatterplots of angular dispersion for rejected attempts from Experiment 3 (10 L min-
1026 [1] bubble curtain). Values nearer to 1.0 indicate greater directionality. Negative x-axis values
1027 indicate motion towards the barrier, positive x-axis values indicate motion away from the
1028 barrier.